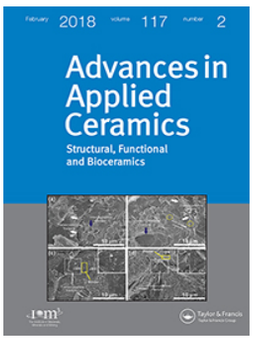

Advances in Applied Ceramics
Structural, Functional and Bioceramics

ISSN: 1743-6753 (Print) 1743-6761 (Online) Journal homepage: http://www.tandfonline.com/loi/yaac20

Glass-ceramic proppants from sinter-crystallisation of waste-derived glasses

Nicoletta Toniolo, Acacio Rincon Romero, Mauro Marangoni, Mohammed Binhussain, Aldo R. Boccaccini & Enrico Bernardo

To cite this article: Nicoletta Toniolo, Acacio Rincon Romero, Mauro Marangoni, Mohammed Binhussain, Aldo R. Boccaccini & Enrico Bernardo (2018) Glass-ceramic proppants from sinter-crystallisation of waste-derived glasses, Advances in Applied Ceramics, 117:2, 127-132, DOI: 10.1080/17436753.2017.1394019

To link to this article: https://doi.org/10.1080/17436753.2017.1394019

ADVANCES IN APPLIED CERAMICS, 2018
VOL. 117, NO. 2, 127–132
https://doi.org/10.1080/17436753.2017.1394019

The Institute of Materials, Minerals and Mining
Taylor & Francis
Taylor & Francis Group

Glass-ceramic proppants from sinter-crystallisation of waste-derived glasses

Nicoletta Toniolo[a,b], Acacio Rincon Romero [a], Mauro Marangoni[a], Mohammed Binhussain [c], Aldo R. Boccaccini [b] and Enrico Bernardo [a]

[a]Dipartimento di Ingegneria Industriale, University of Padova, Italy; [b]Institute of Biomaterials, University of Erlangen, Germany; [c]National Program for Advanced Materials and Building System, KACST, Riyadh, Saudi Arabia

ABSTRACT

The present investigation aims at evidencing the feasibility of glass-ceramic spheres by sinter-crystallisation of fine glass powders (<100 μm), in turn obtained by the melting of inorganic waste, such as red mud from Bayer process or municipal solid waste incinerator fly ash, or low-cost minerals. While dense and highly crystallised monoliths may be achieved by sintering pressed glass powders just at the glass crystallisation temperature (T_C), applying fast heating and short holding times, dense glass-ceramic beads could be obtained only by firing well above T_c ($T_c + 100$°C). An increased sintering temperature was applied in order to enhance the viscous flow and promote the spheroidisation of powder clusters, previously formed by casting fine powders on a rotating drum. The high degree of crystallinity and the uniform microstructure were found to contribute positively to the mechanical properties (compressive strength exceeding 120 MPa, for beads with a diameter of 1 mm, approximately).

ARTICLE HISTORY
Received 9 June 2017
Accepted 25 September 2017

KEYWORDS
Glass-ceramics; sintering; crystallisation; hydraulic fracking; proppant

Introduction

The so-called 'hydraulic fracturing' has been extensively applied for the last 10 years, especially in the U.S.A. [1], for oil and natural gas extraction from shale rock, in very deep wells. This technology relies on the use of beads with particularly high compressive strength, known as 'proppants', pumped with water and chemicals in the wells. Cracks formed in the rock walls are kept open by the insertion of the beads, helping the escape of oil and gas previously trapped between the thin laminae of the same shale rocks. Huge amounts of proppants, in form of sands or artificial beads, along with huge amounts of water and chemicals, are used per well [2], so that several controversies may arise.

Besides risks of groundwater contamination and air quality degradation, a controversy specifically involves the manufacturing of artificial beads. In fact, ceramic beads provide enhanced service, compared to sand, due to uniform size and shape and higher strength [3]; however, high performance proppants, such as alumina-based proppants, are particularly disputable, for the use of commodity minerals (e.g. bauxite) in an application without any recycling/recovery potential [4]. The use of alternative, low-cost raw materials is highly advisable, and glass, for the possibility of incorporating many oxides, of different origin – from refined minerals as well as from a number of inorganic waste – constitutes an undoubted reference [5].

Some proppants actually consist of glass beads [5]. When thinking at high strength solutions, however, the reference to glass-ceramics is far more appropriate [6,7]. In fact, when properly formulated, a glass may undergo a significant crystallisation, with formation of silicate and alumino-silicate crystals in a residual glass matrix; cracks propagating in the brittle glass matrix are typically subjected to remarkable crack deflection at glass–crystal interfaces [8].

The manufacturing of glass-ceramic beads implies processing costs that could compromise the overall sustainability of waste-derived materials instead of other ceramic proppants. In particular, both shaping and crystallisation are quite delicate. The crystallisation of glass beads, i.e. starting from bulk glass pieces, may require long holding times at temperature above the glass transition temperature [8]. Pores and other defects in glass beads remain 'frozen' in a matrix of particularly high viscosity, given the formation of crystalline rigid inclusions; the shaping of glass-ceramic proppants in form of spherical beads requires the adoption of a specifically designed spheroidisation apparatus, starting from molten glass [9].

The present investigation is not intended at discussing the overall sustainability of fracking technology, but at improving the environmental sustainability in terms of materials. We will focus specifically on presenting an alternative, low-cost technology for the obtainment of nearly spherical glass-ceramic proppants, based on

CONTACT Enrico Bernardo enrico.bernardo@unipd.it

glass viscous flow sintering with concurrent crystallisation, i.e. 'sinter-crystallisation'.

As previously observed, sinter-crystallisation has distinctive advantages compared to other technologies for glass-ceramic manufacturing, in terms of sustainability. First, when applying the sintering route, there is no need to refine the melt before casting into a frit, thus reducing cost and gaseous emissions; the vitrification may be conducted in small plants and in particularly short times, favouring the immobilisation of components which could vaporise with longer heat treatments. Second, a relatively high degree of crystallisation may be achieved in very short times, the surface of glass being a preferred site for nucleation [10–13]. In general, powdered glass is easier to devitrify than bulk glass with the same composition, so that nucleating agents are not needed [8]. In some cases, the holding time at the sintering temperature may not exceed 30 min, being also accompanied by very fast heating rates (even 'direct heating' is possible, that is the direct insertion of glass powder compacts in the furnace directly at the sintering temperature), thus configuring a 'fast sinter-crystallisation' [14].

The most significant challenge of the present paper (and the related sinter-crystallisation concept) concerns the shape. Ground glass powders may be easily pressed in the form of regular tiles; the crystallisation, generally starting at the contact points between adjacent glass granules, gives a pleasant visual appearance to the products, after light polishing [14], but it also impedes extensive viscous collapse (near net shape may be achieved, given a quite uniform shrinkage). We will show that the obtainment of spheroids depends on the engineering of the sintering-crystallisation balance.

Experimental procedure

The chemical composition of three starting glasses is shown in Table 1. The composition of commercial sinter-crystallised glass-ceramics (Neoparies™) [8,15] was chosen as a reference for the first glass, termed WM1; besides optimum properties for sinter-crystallisation (discussed later), this composition is quite easy to be achieved starting from mixture of waste [14]. The second glass, termed WM2, was considered as a variant, specifically exploited for white glass-ceramics [16]. Both glass batches were formulated using natural raw materials from Saudi Arabia and a limited amount of pure chemicals (e.g. ZnO, borax and K_2CO_3). The third glass, termed VRM, was actually mostly derived from inorganic waste, in form of fly ash from lignite combustion (obtained from the Public Power Industry of Greece, Megalopolis plant), red mud (by-product of the Bayer process for alumina production, obtained from Aluminium of Greece) and soda-lime cullet, in analogy with a previous investigation [17].

The raw materials were first dried and homogenised by ball milling in an agate jar for 30 min at 300 rev min^{-1} and finally melted in kyanite refractory crucibles at 1400°C for 90 min in static air. The molten glasses did not corrode the crucible, so that the chemical composition was not altered. After achieving complete melting of the raw materials, the melts were poured into water to produce glass frits. The drastic quenching provided a number of fragments that were successively dried at 80°C overnight, ball milled (30 min at 400 rev min^{-1}) and sieved to obtain particles with a size below 90 μm. All glasses, in form of fine powders, were subjected to differential thermal analysis (DTA/TGA, STA 409; Netzsch-Gerätebau GmbH, Selb, Germany, operated at 10°C min^{-1} in static air).

'Green' glass granules were obtained by means of a specifically designed 'snow-balling' apparatus. Fine glass powders were first cast on a Teflon drum, spinning at 400 rev min^{-1} on an oblique axis, as shown by Figure 1. A binding solution was added dropwise (0.5 g binder, consisting of distilled water with 5% PVA, for 4 g glass powders) during rotation. Dry particles progressively attached to wet particles upon rolling; the same rolling readily transformed particle clusters in quite regular spherical granules. After most of the dry powders were consolidated, the

Table 1. Chemical composition of the starting glasses (wt-%).

	WM1	WM2	VRM Waste-derived glass	Coal fly ash	Red mud
Oxides					
SiO_2	62.0	56.9	44.8	49.4	7.8
Al_2O_3	7.1	5.1	14.9	22.7	17.1
CaO	19.4	19.6	22.4	8.9	11.7
MgO	3.4	7.9	2.7	1.6	0.6
Na_2O	2.4	2.8	2.7	0.9	3.2
K_2O	3.5	1.4	0.9	1.4	0.1
B_2O_3	1.2				
TiO_2	0.6	0.1	1.7	1.1	5.1
ZnO		5.7			
Fe_2O_3			9.7	7.4	44.1
Formulation	Natural raw materials (oxides and carbonates)		31% Coal fly ash 16% red mud 11% recycled soda-lime glass + natural raw materials		

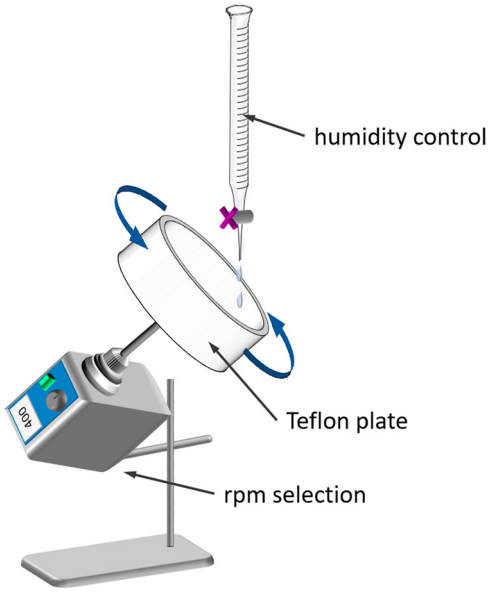

Figure 1. Scheme of the 'snow-ball spheroidisation' apparatus adopted for the manufacturing of 'green' glass granules.

rotation could be arrested and the granules could be sieved. The subsequent firing experiments were applied to granules with diameter from 1 to 1.5 mm, after drying (80°C, overnight).

The firing of granules was conducted on refractory plates coated with a carbon black powder bed, to avoid refractory-glass adhesion. After a stage in a first muffle furnace, at 300°C, for 60 min (10°C min^{-1} heating rate), aimed at binder burn-out, the granules were directly inserted in a second muffle furnace, preheated at 1050°C, and left for 30 min. The microstructural evolution was 'frozen' by rapid cooling of the furnace from 1050 to 700°C (the heating was arrested just after 30 min at the maximum temperature and the cooling was forced by keeping the furnace door partially open), followed by natural cooling.

The density of the beads was determined geometrically and by weighing with an analytical balance. The apparent and true densities of the various specimens were measured by means of a gas pycnometer (Micromeritics AccuPyc 1330, Norcross, GA), operating with He gas on samples in bulk and powder form.

Glass-ceramic granules were finally subjected to compressive testing using an Instron 1121 UTS instrument (Instron, Danvers, MA) on at least 20 spheres for each sample type (with a diameter of approx. 0.9 mm); the granules were pressed between SiC discs with a crosshead speed of 1 mm min^{-1}. Broken pieces were studies by means of both optical and scanning electron microscopy (SEM-ESEM Quanta 200, FEI Company, Eindhoven, The Netherlands).

Powdered glass-ceramics were investigated by X-ray diffraction (Bruker D8 Advance, Karlsruhe, Germany), employing CuKα radiation (0.15418 nm) and collecting data in the range $2\theta = 10–70°$ (0.05° steps and 5 s counting time). The identification was performed by means of a semi-automatic software package (Match!, Crystal Impact GbR, Bonn, Germany), supported by data from PDF-2 database (ICDD-International Centre for Diffraction Data, Newtown Square, PA).

Results and discussion

The three glasses exhibited a quite similar thermal behaviour, as illustrated by the DTA plots in Figure 2. The glass transition temperature (T_g) is practically the same for all (≈650°C), and also the crystallisation temperature (T_c) falls in a limited range (900–950°C). The intensity of the crystallisation exothermic peak increases (we tested nearly the same amount of fine glass powders, for each plot) passing from WM1 to VRM. The endothermic effects above 1100°C are also different, reasonably due to changes in the developed crystal phases.

In any case, the gap between the transition temperature and the crystallisation temperature is quite large; for sintering treatments at the crystallisation temperature, the viscous flow may be quite abundant, with a good densification, as previously observed for the development of glass-ceramic tiles [14,17]. However, this condition is generally verified for tiles developed starting from pressed powders, i.e. from already densified green bodies; the adopted spheroidisation method implied a revision of the viscous flow/crystallisation balance.

More precisely, the firing at 1050°C, at least 100°C above T_c, was specifically intended to favour the viscous flow, in turn aimed not only at densification, but also to achieve a spherical shape, as an effect of the reduction of specific surface. Figure 3 testifies the effective achievement of the desired shape, despite some defects, such as 'bumps' on the surface and internal pores.

The bumps are likely due to the collapse of surface bubbles, caused by some gas evolution, responsible

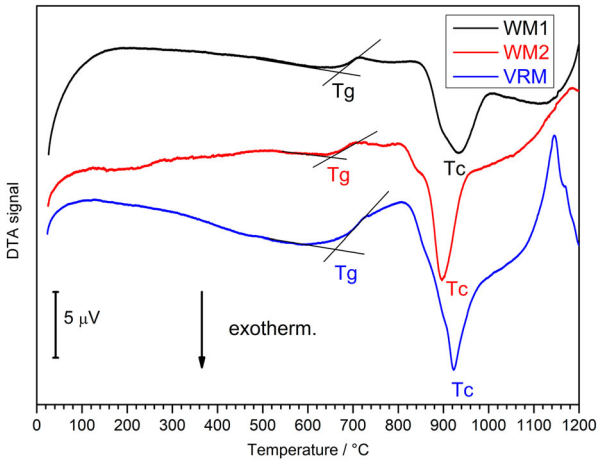

Figure 2. DTA plots of fine glass powders of different composition.

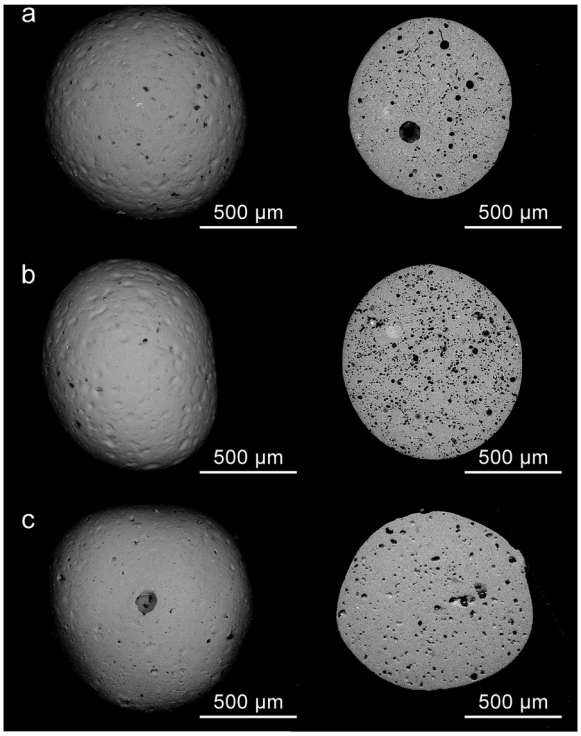

Figure 3. Examples of glass-ceramic beads (left: overall appearance; right: cross-section details) derived from: (a) WM1; (b) WM2; (c) VRM.

also for the internal pores. The fast vitrification process reasonably caused the trapping of some gasses (from the same vitrification reactions, involving the decomposition of carbonates, hydrated salts, etc.) dissolved in the glass structure. We cannot exclude, for the bubbles at the surface of VRM glass-derived beads (Figure 3(c)), some interaction of glass with the carbon black bed, particularly between ferric oxide, undergoing reduction, and C (Fe_2O_3 +× C→(FeO,Fe_3O_4) + CO). WM2 and VRM, crystallising at lower temperature or more intensively (given the peaks in Figure 2) than WM1, allowed for some control of the porosity: unlike WM1-derived beads, the resulting glass-ceramic had a quite homogeneously distributed residual porosity. The precipitation of crystal inclusions, with significant increase of viscosity, reasonably impedes the coalescence of small pores into bigger ones (like that visible in the cross-section of WM1 glass-ceramic, in Figure 3(a)).

The substantial crystallisation is further evidenced by both SEM (polished cross-sections) and X-ray diffraction analysis, reported in Figures 4 and 5, respectively. From Figure 4(a,b) we can note that, passing from WM1 to WM2, the above mentioned increase of viscosity could depend also on the morphology of crystals inclusions; in particular, WM2 led to more elongated crystal inclusions. The sensitivity of WM2 to surface crystallisation is testified by the intensive crystallisation around the pores (Figure 4(b)). Elongated and well-distributed crystals are also found for VRM-derived glass-ceramic (Figure 4(c)).

The developed glass-ceramics actually feature different silicate phases. Passing from WM1 to WM2, the slight compositional variation led to a remarkable change in the phase assemblage. The WM1-derived glass-ceramic is characterised by the formation of wollastonite ($CaSiO_3$, PDF#75-1396) and diopside ($CaMgSi_2O_6$, PDF#75-1092); while the latter phase remains in WM2-derived glass-ceramic, wollastonite is replaced by akermanite ($Ca_2MgSi_2O_7$, 87-0048). This may be justified not only by the enhanced MgO content, but also by the presence of ZnO; in fact, akermanite belongs to the vast group of melilites, including both akermanite and Zn-containing variant (hardystonite, $Ca_2ZnSi_2O_7$) [18,19]. The detected akermanite phase is likely a solid solution (hardly distinguishable, in terms of diffraction peaks, from pure akermanite).

Diopside may be considered as a reference even for VRM-derived glass-ceramic beads. In fact, diopside belongs to the pyroxene group; compared to pure diopside, pyroxenes may feature substitutions, in the Ca^{2+}, Mg^{2+} and Si^{4+} sites, with Fe^{2+}, Fe^{3+} and Al^{3+} ions [8], similarly to what was recognised as the main phase of VRM-derived glass-ceramic ($Ca(Mg_{0.6}Fe_{0.2}Al_{0.2})(Si_{1.5}Al_{0.5})O_6$, PDF#72-1379). Wollastonite is again present, with a third phase represented by labradorite, i.e. a Na-Ca alumino-silicate of the feldspar group ($Na_{0.5}Ca_{0.5}Al_{1.5}Si_{2.5}O_8$, PDF#78-0434).

The remarkable crystallisation enhanced the mechanical strength, validly counterbalancing the above discussed defects. As evidenced by Figure 6(a), crystal inclusions caused a significant crack deflection; the failure, in all cases, as shown by Figure 6(b), occurred in a 'graceful' way, i.e. the fragments could retain the

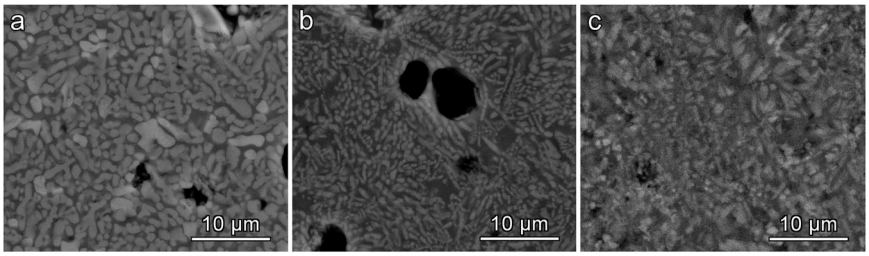

Figure 4. SEM micrographs of polished cross-sections of glass-ceramic beads derived from: (a) WM1; (b) WM2; (c) VRM.

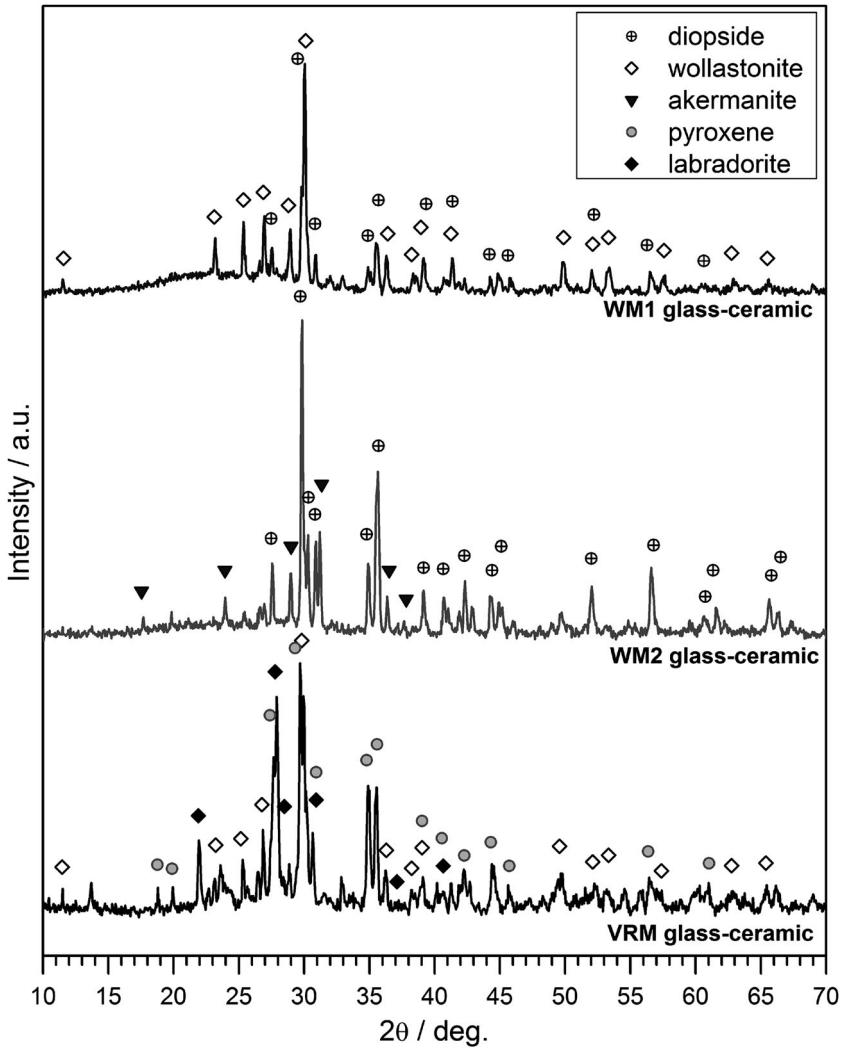

Figure 5. X-ray diffraction patterns of the developed glass-ceramics.

propping action, when in operation (this is recognised as a fundamental condition for high performance proppants [20]).

Table 2 provides a summary of physical and mechanical properties of the obtained glass-ceramic beads. The residual porosity, in VRM-derived beads, is quite high. However, the amount of open porosity is low, like in the other two samples. The characteristic strength well exceeds 100 MPa, in all cases, and it is quite remarkable, considering the dimensions. The Weibull's statistics, in fact, allows for the prediction of the strength for smaller sizes, closer to that of commercial proppants (we considered a scale factor for strength equal to $(V/V_C)^{1/m}$, where V is the average volume of experimental samples and V_C is the volume of hypothetical samples with a diameter of 0.6 mm). The predicted values well agree with the strength values of commercial proppants [21,22].

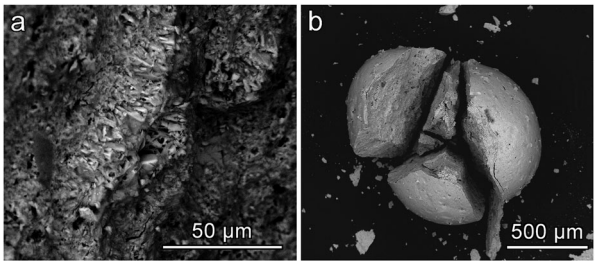

Figure 6. (a) Rough fracture surface of VRN-derived glass-ceramic bead; (b) evidence of 'graceful failure' in WM2-derived glass-ceramic bead.

The present investigation is probably only a starting point for sintered glass-ceramic proppants. Additional efforts will be reasonably dedicated, in the future, to the manufacturing and characterisation of finer beads (in order to validate the predictions from Weibull's statistics). The enhancement of densification (e.g. studying the impact of the refining of the glass melt, or controlling the heating rate, or even mixing a glass undergoing significant crystallisation with one not prone at all to devitrification, filling pores by viscous flow [14]) may be studied as well. Finally, we may envisage the development of glasses, of similar overall composition, but developed by mixing other types of industrial waste.

Table 2. Physical and mechanical properties of the obtained glass-ceramic beads.

Sample	Geometrical density (g cm^{-3})	Total porosity	Open porosity [% of total porosity]	Weibull's parameters		Prediction
				σ_0 (MPa)	m Weibull's modulus	σ_0 for $\varphi = 0.6$ mm (MPa)
WM1	2.30 ± 0.03	3.6	0.7 [19%]	135	6.8	169
WM2	2.73 ± 0.03	3.5	1.1 [31%]	160	4.1	233
VRM	2.62 ± 0.03	11	0.8 [7%]	144	9.0	171

Conclusions

We may conclude that:

- Sinter-crystallisation has a great potential for the manufacturing of a new generation of low-cost glass-ceramic proppants;
- Sinter-crystallisation can be applied to glasses with a quite large compositional variety, given a quite wide gap between softening and crystallisation;
- The spheroidisation is a consequence of enhancement of viscous flow, upon sintering well above the glass crystallisation temperature.

Acknowledgements

EB acknowledges Prof Yiannis Pontikes (KU Leuven, Belgium) for supplying red mud and lignite combustion fly ash.

Disclosure Statement

No potential conflict of interest was reported by the authors.

Funding

This project has received funding from the European Union's Horizon 2020 research and innovation programme under H2020 Marie Sklodowska Curie Actions grant agreement No. 642557 (CoACH – Advanced Glasses, Composites and Ceramics for High Growth Industries European Training Network (ETN)). EB and MM thank King Abdulaziz City for Science and Technology (KACST), Saudi Arabia, for support and funding through grant No. 32-639.

ORCID

Acacio Rincon Romero http://orcid.org/0000-0003-0350-8304
Mohammed Binhussain http://orcid.org/0000-0002-2553-0142
Aldo R. Boccaccini http://orcid.org/0000-0002-7377-2955
Enrico Bernardo http://orcid.org/0000-0003-4934-4405

References

[1] Gandossi L. An overview of hydraulic fracturing and other formation stimulation technologies for shale gas production. Eur Comm Jt Res Cent Technol Reports. 2013.
[2] Gallegos T.J, Varela B.A. Trends in hydraulic fracturing distributions and treatment fluids, additives, proppants, and water volumes applied to wells drilled in the United States from 1947 through 2010: Data analysis and comparison to the literature, scientific investigations report 2014-5131 (2015).
[3] Liang F, Sayed M, Al-Muntasheri GA, et al. A comprehensive review on proppant technologies. Petroleum. 2016;2:26–39.
[4] Zhao J, Liu Z, Li Y. Preparation and characterization of low-density mullite-based ceramic proppant by a dynamic sintering method. Mater Lett. 2015;152:72–75.
[5] Hellmann JR, Scheetz BE, Luscher WG, et al. Proppants for shale gas and oil recovery. Am Ceram Soc Bull. 2014;93:28–35.
[6] Economides MJ, Martin T. Modern fracturing: enhancing natural gas production. Houston (TX): Energy Tribune Publishing Inc.; 2017.
[7] Mader D. Hydraulic proppant fracturing and gravel packing. Amsterdam: Elsevier; 1989.
[8] Höland W, Beall GH. Glass-ceramic technology (2nd edition). Hoboken (NJ): John Wiley & Sons; 2012.
[9] Koseski R.P., Hellmann J.R., Scheetz B.E. Treatment of melt quenched aluminosilicate glass spheres for application as proppants via devitrification processes. United States patent US 8,359,886. 2013.
[10] Müller R, Zanotto ED, Fokin V. Surface crystallization of silicate glasses: nucleation sites and kinetics. J Non-Cryst Sol. 2000;274:208–231.
[11] Prado MO, Zanotto ED. Glass sintering with concurrent crystallization. C R Chim. 2002;5:773–786.
[12] Francis A, Rawlings R, Sweeney R, et al. Crystallization kinetic of glass particles prepared from a mixture of coal ash and soda-lime cullet glass. J Non Cryst Sol. 2004;333:187–193.
[13] Hernández-Crespo MS, Romero M, Rincón JM. Nucleation and crystal growth of glasses produced by a generic plasma arc-process. J Eur Ceram Soc 2006;26:1679–1685.
[14] Bernardo E. Fast sinter-crystallization of a glass from waste materials. J Non Cryst Sol. 2008;354:3486–3490.
[15] http://www.negb.co.jp/en (accessed 2017 Apr)
[16] Marangoni M, Nait-Ali B, Smith D, et al. White sintered glass-ceramic tiles with improved thermal insulation properties for building applications. J Eur Ceram Soc. 2017;37:1117–1125.
[17] Bernardo E, Esposito L, Rambaldi E, et al. Sintered esseneite–wollastonite–plagioclase glass–ceramics from vitrified waste. J Eur Ceram Soc. 2009;29:2921–2927.
[18] Kaminskii A, Belokoneva E, Mill B, et al. Crystal structure, absorption, luminescence properties, and stimulated emission of Ga gehlenite ($Ca_{2-x}Nd_xGa_{2x}Si_{1-x}O_7$). Phys Stat Sol. 1986;97:279–290.
[19] Giuli G, Bindi L, Bonazzi P. Rietveld refinement of okayamalite, $Ca_2SiB_2O_7$: structural evidence for the B/Si ordered distribution. Am Mineral. 2000;85:1512–1515.
[20] Koseski R.P. Manipulation of microstructure, phase evolution and mechanical properties by devitrification of andesite for use as proppant [PhD dissertation]. 2008.
[21] http://www.carboceramics.com (accessed 2017 Apr)
[22] http://www.proppants.saint-gobain.com (accessed 2017 Apr)